www.nature.com/aps

Acta Pharmacologica Sinica

ARTICLE

Ginsenoside Rb1 alleviates diabetic kidney podocyte injury by inhibiting aldose reductase activity

Jia-yi He[1,2], Quan Hong[1], Bi-xia Chen[1,2], Shao-yuan Cui[1], Ran Liu[1], Guang-yan Cai[1], Jiao Guo[2] and Xiang-mei Chen[1,2]

Panax notoginseng, a traditional Chinese medicine, exerts beneficial effect on diabetic kidney disease (DKD), but its mechanism is not well clarified. In this study we investigated the effects of ginsenoside Rb1 (Rb1), the main active ingredients of *Panax notoginseng*, in alleviating podocyte injury in diabetic nephropathy and the underlying mechanisms. In cultured mouse podocyte cells, Rb1 (10 μM) significantly inhibited high glucose-induced cell apoptosis and mitochondrial injury. Furthermore, Rb1 treatment reversed high glucose-induced increases in Cyto *c*, Caspase 9 and mitochondrial regulatory protein NOX4, but did not affect the upregulated expression of aldose reductase (AR). Molecular docking analysis revealed that Rb1 could combine with AR and inhibited its activity. We compared the effects of Rb1 with eparestat, a known aldose reductase inhibitor, in high glucose-treated podocytes, and found that both alleviated high glucose-induced cell apoptosis and mitochondrial damage, and Rb1 was more effective in inhibiting apoptosis. In AR-overexpressing podocytes, Rb1 (10 μM) inhibited AR-mediated ROS overproduction and protected against high glucose-induced mitochondrial injury. In streptozotocin-induced DKD mice, administration of Rb1 (40 mg·kg^{-1}·d^{-1}, ig, for 7 weeks) significantly mitigated diabetic-induced glomerular injuries, such as glomerular hypertrophy and mesangial matrix expansion, and reduced the expression of apoptotic proteins. Collectively, Rb1 combines with AR to alleviate high glucose-induced podocyte apoptosis and mitochondrial damage, and effectively mitigates the progression of diabetic kidney disease.

Keywords: diabetickidney disease; ginsenoside Rb1; podocyte apoptosis; oxidative stress; aldose reductase; Cyto *c*; NOX4; eparestat

Acta Pharmacologica Sinica (2022) 43:342–353; https://doi.org/10.1038/s41401-021-00788-0

INTRODUCTION

Diabetic kidney disease (DKD) is the strongest predictor of mortality in diabetic patients and the main cause of end-stage renal disease [1, 2]. The early pathological changes in diabetic nephropathy mostly occur in glomeruli and include glomerular basement membrane (GBM) thickening and glomerular hypertrophy [3]. Podocytes, which form an important part of the glomerular filtration barrier, play an essential role in maintaining the function and structure of the glomerulus [4, 5]. Most structural and functional podocyte-related disorders, such as the disappearance of foot processes (FPs), hypertrophy, shedding, and apoptosis, can lead to the occurrence of proteinuria [6]. In recent years, the critical effects of podocyte injury in the initiation and progression of DKD have attracted great attention, and it is generally believed that podocyte injury might be a new target for the treatment of kidney disease [7]. Therefore, alleviating podocyte injury might be a key factor in the future relief of DKD.

Panax notoginseng, a perennial herb of the family Acanthaceae, is one of the most commonly used traditional Chinese medicine (TCM), and its main active ingredients include saponin, flavonoids, amino acids, and sterols [8, 9]. Recent studies have found that *Panax notoginseng* exerts anti-cerebral-ischemia, anti-arrhythmic, anti-oxidant, anti-atherosclerosis, lipid-lowering, and other pharmacological effects, and other recent evidence has suggested that *Panax notoginseng* saponins (PNS) exert an inhibitory effect on inflammatory cytokines, fibrosis-related protein expression, and podocyte apoptosis in diabetic rats [10–13]. PNS can alleviate the STZ-induced apoptosis of diabetic rat podocytes via TGF-β/p38 MAPK signaling [14]. Zhou et al. also found that PNS treatment for 10 weeks can effectively improve glomerular mesangial hyperplasia and maintain the number of podocytes [15], but the identity and specific mechanism of action of the effective components are unclear.

Therefore, we selected the two saponins with the highest abundance in *Panax notoginseng*, ginsenoside Rb1, and Rg1, and the notoginsenoside-specific notoginsenoside R1 to assess whether these monomers may serve as a promising therapeutic candidate for DKD. Some studies have found that in 3T3-L1 cells, ginsenoside Rb1 can stimulate the fat formation and insulin-mediated glucose uptake and promote basal glucose transport

[1]Department of Nephrology, First Medical Center of Chinese PLA General Hospital, Nephrology Institute of the Chinese People's Liberation Army, State Key Laboratory of Kidney Diseases, National Clinical Research Center for Kidney Diseases, Beijing Key Laboratory of Kidney Disease Research, Beijing 100853, China and [2]Guangdong Metabolic Diseases Research Center of Integrated Chinese and Western Medicine; Key Laboratory of Glucolipid Metabolic Disorder, Ministry of Education of China, Institute of Chinese Medicine, Guangdong Pharmaceutical University; Guangdong TCM Key Laboratory for Metabolic Diseases, Guangzhou 510006, China
Correspondence: Jiao Guo (gyguoyz@163.com) or Xiang-mei Chen (xmchen301@126.com)
These authors contributed equally: Jia-yi He, Quan Hong

Received: 9 May 2021 Accepted: 29 September 2021
Published online: 22 November 2021

and GLUT1 and GLUT4 translocation through the insulin-like signaling pathway, which reduces the glucose level and induces anti-diabetic effects [16, 17]. Ma et al. found that ginsenoside Rg1 can inhibit TGF-β1 expression in diabetic nephropathy rats and thereby relieves renal fibrosis [18].

MATERIALS AND METHODS

Mouse model

Male FVB mice were purchased from Beijing HFK Bioscience. Diabetes was induced in 8-week-old mice through the intraperitoneal administration of STZ (dissolved in 0.1 M Citrate buffer, pH 4.5, S0103, Sigma, US) at 50 mg/kg after 4–6 h of food deprivation each day for 5 consecutive days. Citrate buffer-injected mice served as non-diabetic controls. Twenty-one-week-old mice were treated with either vehicle or ginsenoside Rb1(112127, J&K Scientific, Beijing, China) by oral gavage at a dose of 40 mg/kg body weight per day for 7 weeks. The blood glucose, urinary albumin, and body weight were monitored every 2 weeks. At 28 weeks of age, the mice were anesthetized and sacrificed by intraperitoneal injection of 1% sodium pentobarbital (45 mg/kg), and their blood, urine, and kidney tissues were collected. This experimental research plan has been approved by the Animal Ethics Committee of the PLA General Hospital before the start of the experiment (2018-x14-23). All of the animal care and experimental procedures complied with the guidelines for the Care and Use of Laboratory Animals published by the United States National Institutes of Health (NIH publication, 2011 Revision).

Measurement of blood glucose and urine albumin

The blood glucose level in blood samples collected from the tail vein every 2 weeks was measured and the level of urine albumin was determined using a commercial enzyme-linked immunosorbent assay kit (E99-134,Bethyl Laboratory Inc., Houston, TX, USA). The urine creatinine levels in the same samples were measured using the Creatinine Colorimetric Assay Kit (500701, Cayman Chemical, Ann Arbor, MI, USA). For the determination of UAE, urine samples were collected for 24 h using metabolic cages.

Kidney histology

The kidney samples were fixed in 10% formalin, embedded in paraffin, and sectioned to 4 μm thickness. The sections were stained with periodic acid–Schiff (PAS) for analysis of the glomerular area and mesangial matrix expansion. Images were obtained at ×400 magnification using a Zeiss AX10 microscope (Carl Zeiss Jena, Toronto, Canada). The relative mesangial area was expressed as the percentage of the mesangial-to-glomerular surface area. The degree of mesangial expansion was quantified based on a minimum of 10 glomeruli per section at ×400 magnification in a blinded manner. The mouse glomerular volume (GV) was calculated from the cross-sectional area using the formula

$$GV = \beta/k \times (GA)^{3/2}$$

where $\beta =$ the shape coefficient for a sphere and $k = 1.1$ is the size distribution coefficient. For transmission electron microscopy (TEM), kidney cortex samples fixed in 2.5% glutaraldehyde were divided into sections and mounted on a copper grid, and images were acquired using the Hitachi H7650 Microscope (Hitachi, Tokyo, Japan) as previously described [19]. The FP effacement and GBM width were quantified from digitized TEM images using ImageJ software, as previously described [20]. For quantification of the GBM thickness, a mean of 55 measurements (GBM length >600 mm) were obtained from each mouse (from podocytes to the endothelial cell membranes) at random sites in the cross-section in which the GBM was optimally displayed. The same glomeruli were used to obtain the degree of podocyte effacement, which was defined as the percentage of the total glomerular capillary surface area over which the podocyte foot processes were effaced.

Cell culture

The conditionally immortalized mouse podocyte cell (MPC) line was kindly provided by the Type Culture Collection of the Chinese Academy of Sciences (Shanghai, China). Mouse podocyte cells (MPCs) were propagated at 33 °C in RPMI-1640(10-040-CVRC, Corning, US) medium supplemented with 10% FBS(0500, Sciencell, US), penicillin-streptomycin solution (0513, Sciencell, US), and 10 U/mL recombinant mouse IFN-γ (I4777, Sigma, US). For the induction of differentiation, the podocytes were grown on plates coated with collagen-I (9007-34-5, Sigma, US) at 37 °C in the absence of IFN-γ for 5 days. After differentiation, the cells were treated with normal glucose (5 mM D-glucose), a high concentration of glucose (30 mM D-glucose), or mannitol (5 mM D-glucose +25 mM mannitol).

AR activity assay

MPC stimulated with high glucose for 72 h was used to detect AR activity (JM9156, HEPENG Biological, Shanghai, China). The protein concentration of the cell sample was detected after lysis and diluted to 2 μg/μL then different doses of Rb1 was added to the lysed protein for subsequent detection. After the 96-well plate was marked, 150 μL of buffer solution was transferred to each well of the plate, and 20 μL of reaction and substrate solutions were then added. The plate was gently shaken and incubated at 25 °C for 3 min. Subsequently, 10 μL of negative solution or the test sample (20 μg of protein) was added to the corresponding wells. Before reading, the microplate reader was set to 25 °C, wavelength at 340 nm, and was read every 2 min for 6 times, a total of 10 min. The plate was then gently shaken and detected using a microplate reader (Tecan), and readings were obtained at 0 and 10 min to calculate the AR activity of the sample. The above reaction reagents are all provided in the kit.

Western blotting

For protein extraction, the whole tissue/cell pellets were dissolved in RIPA buffer. Fifty micrograms of protein were separated by 10% SDS-PAGE and transferred onto polyvinylidene difluoride (PVDF) membranes. After 1 h of blocking with 5% skimmed milk powder, the PVDF membrane was incubated with the primary antibodies overnight at 4 °C. The primary antibodies against NOX4 (ab133303, Abcam, US), Cyto *c* (ab133504, Abcam, US), cleaved Caspase 3 (ab2302, Abcam, US), active Caspase 9 (ab2325, Abcam, US), AR (sc-166918, Santa Cruz, US), cleaved PARP-1 (ab32064, Abcam, US) and β-actin (66009,Proteintech, US) were diluted in 5% BSA. The PVDF membrane was then incubated with HRP-tagged secondary antibodies (A0216/A0208, Beyotime, China) at room temperature for 1–2 h, and the signals were detected with the Western blot reagent ECL. ImageJ software was used for density analysis, and the IntDen value obtained was used to compare each group for statistical analysis.

Flow cytometry

Annexin V, FITC Apoptosis Detection Kit (AD10, Dojindo, Shanghai, China) was used to detect apoptosis, and the steps were as follows. 1× Annexin V Binding Solution was prepared to obtain a cell suspension with a final concentration of 1×10^6 cells/mL, and 100 μL was transferred into a new microtube. Five microliters of Annexin V conjugated to FITC were then added to the cell suspension, and 5 μL of the PI solution was then added. After incubation at room temperature for 15 min in the dark, 400 μL of 1× Annexin V Binding Solution was added, and a flow cytometer (Beckman Coulter) was used for detection within 1 h. Sample was added to flow cytometer for detection, with excitation wavelength

Ex = 488 nm and emission wavelength Em = 530 nm. The green fluorescence of Annexin V-FITC was detected by the FITC channel; the red fluorescence of PI was detected by the PI channel.

MitoSOX mitochondrial superoxide indicator

Dilute the 5 mM MitoSOX™ reagent stock solution (M36008, Molecular Probe, UK) in the suitable buffer to make a 5 μM MitoSOX™ reagent working solution. Apply 200 μL of 5 μM MitoSOX™ reagent working solution to cover cells adhering to the coverslip(s). Incubate cells for 10 min at 37 °C and protect them from light. Wash cells gently three times with a warm buffer. Stain cells with counterstains as desired and mount them in the warm buffer for imaging.

JC-1 mitochondrial membrane potential detection kit

The JC-1 assay (30001, Biotium, US) uses a unique cationic dye (5,5′,6,6′-tetrachloro-1,1′,3,3′-tetraethylbenzimidazolylcarbocyanine iodide) to detect loss of mitochondrial membrane potential. In apoptotic cells, the mitochondrial membrane potential collapses, and JC-1 cannot accumulate in mitochondria. In these cells, JC-1 remains in the cytoplasm in a green fluorescent monomeric form. Apoptotic cells, showing primarily green fluorescence, are easily differentiated from healthy cells, which show red and green fluorescence. The aggregate red form has absorption/emission maxima of 585/590 nm. The green monomeric form has absorption/emission maxima of 510/527 nm. The steps are as follows: Remove the cell culture media and replace it with JC-1 Reagent working solution sufficient to cover the cells. Incubate the cells in a 37 °C cell culture incubator for 15 min. Remove the media and wash the cells once with PBS or cell culture medium.

Aldose reductase molecular docking method

Molecular docking method (Surflex molecular docking module of Sybyl x-2.1) was used. The crystal structure of the complex formed by human-derived aldose reductase protein and its inhibitor is 5OU0. The crystal structure has an excellent resolution of 0.94 angstroms. The crystal structure comes from the latest excellent journal (2018) Eur J Med Chem 152: 160-174 [21].

At present, the crystal structure of the mouse-derived aldose reductase protein has not been resolved, so the results of homology modeling provided by professional online websites are used. The human source and the mouse source are highly homologous, with 85% amino acid sequence identity. The molecular construction of the natural product Rb1 adopts the "Sketch" module of Sybyl X-2.1, and the 2D structure of the reference is shown in the figure below. However, in the experimental process, it's Rb1 that plays an active role in cells or tissues by removing 2 disaccharide groups. Therefore, the final 3D structure of Rb1 is shown in the figure below, and hydrogenated atomic and Gasteiger-Huckel charge are carried out. Finally, the Sybyl X-2.1 "Powell" energy minimization method was used to optimize the structure. The optimized maximum step length is 1000 steps and the energy gradient is 0.005 kcal/(mol*Å). Treatment of receptor proteins during molecular docking: crystal structures 5OU0 (and mouse-AR) were hydrogenated to atoms and charged with AMBER7 FF99. The surrounding amino acid of the inhibitor AV5 (its full name is 2-[5-(4-chlorophenyl)-3-methyl-1-oxidanylidene-Pyrimido [4,5-c] Quinlin-2-YL], Ethanoic acid) in crystal structure 5OU0 was selected as the active site to graft the inhibitor molecule.

Overexpression of aldose reductase in mouse podocyte

After the cells grow to 80% confluency, PolyJet™ In Vitro DNA Transfection Reagent (SL100688, SignaGen Laboratories, US) was used for transfection. Plasmid DNA was added into the transfection reagent at a ratio of 3:1, and incubated at room temperature for 10 min. Gene expression was detected after transfection for 24-48 h.

Statistical analysis

The data are summarized as the means ± SEMs. The differences among more than 3 groups were analyzed using ANOVA followed by the Bonferroni adjustment for multiple comparisons. The statistical significance of the differences among the two groups was assessed by analysis of variance followed by a *t* test based on a value of $P < 0.05$ using GraphPad Prism software (San Diego, CA, USA).

RESULTS

Ginsenoside Rb1 inhibits podocyte apoptosis in a high-glucose environment

To assess whether high glucose levels increased podocyte damage, the differentiated mouse podocytes were divided into four groups according to the duration of the stimulation (24 h, 48, 72, and 96 h). Hoechst staining revealed that compared with the NG group, podocytes in the HG group showed significant nuclear shrinkage and partial fragmentation, which proved that high glucose can induce podocyte apoptosis (Fig. 1a, b). Fluorescence staining results of JC-1 and MitoSOX showed that high glucose affected mitochondrial membrane potential and promoted ROS generation. These results consistently indicated that high glucose stimulation could damage popocyte function and restrain mitochondrial interference with their daily activities (Fig. 1c–f).

To observe whether panax notoginseng alleviates the effects of high glucose on podocytes and which specific components play a major role, three saponins with higher content in *Panax notoginseng* were used for comparison, namely ginsenoside Rb1, ginsenoside Rg1 and Panax notoginseng R1. The changes of a series of apoptosis-related indexes were measured. The analysis of cleaved Caspase 3 suggested that ginsenosides Rb1 might play a potential role in alleviating high glucose-induced podocyte apoptosis, and this result was also confirmed in TUNEL staining (Fig. 1g–i). To verify the above-described results, FITC, PI flow cytometry was used to assesse the effect of ginsenoside Rb1 on apoptosis of cultured podocytes by flow cytometry and it was revealed that ginsenoside Rb1 treatment for 72 h reduced the apoptosis ratio of podocytes in the presence of a high glucose level (Fig. 1j–l). Taken together, these data show that ginsenoside Rb1 can inhibit the apoptosis of podocytes under high glucose conditions.

Ginsenoside Rb1 improves mitochondrial damage and oxidative stress caused by high glucose

Since the effects of mitochondrial function have been tested before, we hypothesized that glucose overdose also affects mitochondrial morphology. Phalloidin staining confirmed that the HG-induced disorder of the podocyte structure could be alleviated by ginsenoside Rb1 (Fig. 2). Meanwhile, ginsenoside Rb1 was observed to reduce the superoxide production induced by glucose excess and improve the abnormality of mitochondrial membrane potential (Fig. 2b–e).

Since the previous experiment found that Rb1 inhibited cleaved Caspase-3 protein expression, we also verified its effects on the activity and related proteins and found that Rb1 inhibited the activity of Caspase-3 while inhibiting Caspase-9 expression (Fig. 2f–h). Previous evidence has proven that in a high-glucose environment, the NADPH oxidase family can produce excessive ROS, which contributes to the enhancement of oxidative stress and the promotion of podocyte apoptosis [22–25]. Our data showed that a high glucose level can enhance the expression of NOX4, a member of the NADPH oxidase family, to induce excessive ROS production and ultimately cause podocyte damage, which leads to apoptosis. And as shown in Fig. 2i–n, ginsenoside Rb1 can reduce NOX4 expression and its activity, then help relieve the release of Cyto *c* from mitochondria thereby maintaining the structural and functional integrity of mitochondria.

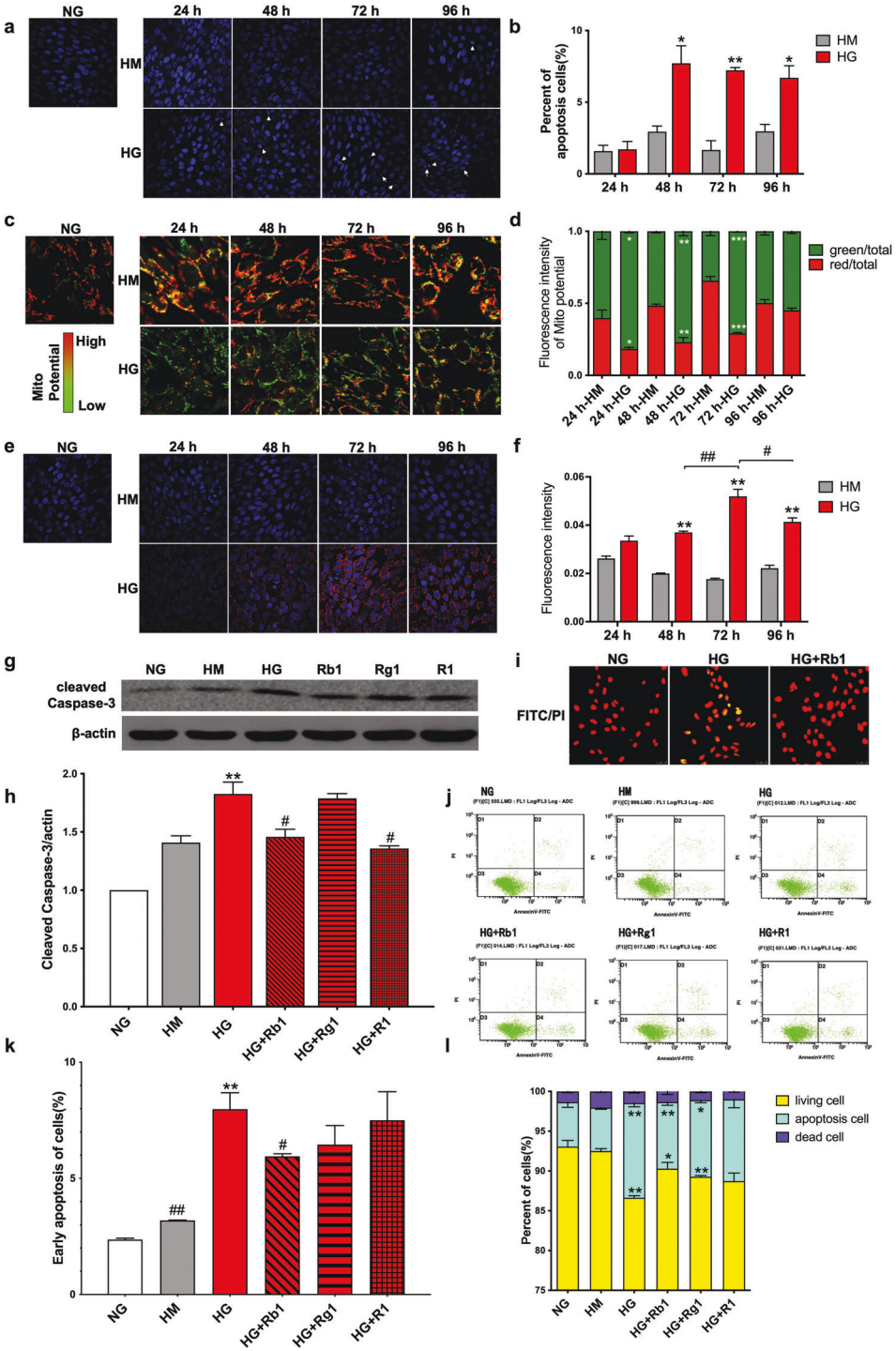

Fig. 1 Ginsenoside Rb1 inhibits podocyte apoptosis in the high glucose environment. a, **b** Representative images of podocyte expression of Hoechst (blue) and their quantification are shown of podocyte with normal glucose (NG), podocyte with mannitol (HM), and podocyte with high glucose (HG). **c**, **d** Representative images of podocytes of mitochondrial membrane potentials and their quantification are shown. **e**, **f** We employed the mitochondrion-specific probe MitoSOX Red to detect changes in ROS levels. Representative images and their quantification are shown. **g**, **h** Representative photographs of cleaved Caspase-3 in Western blots and the quantitative analyses are shown. **i** FITC/PI staining was used to detect the effect of Rb1 on apoptosis. **j**–**l** We used flow cytometry to detect the proportion of podocyte apoptosis, representative pictures, (**k**) the proportion of early apoptotic cells to the total number of cells, and (**l**) the proportion of cells in each category are shown. Data are shown as mean ± SEM. The differences among ≥3 groups were analyzed using ANOVA followed by the Bonferroni adjustment for multiple comparisons. *P* values between groups from unpaired *t* test of variance are as indicated. $^{*}P < 0.05$, $^{**}P < 0.01$, versus NG/HM group. $^{\#}P < 0.05$, $^{\#\#}P < 0.01$, versus HG group.

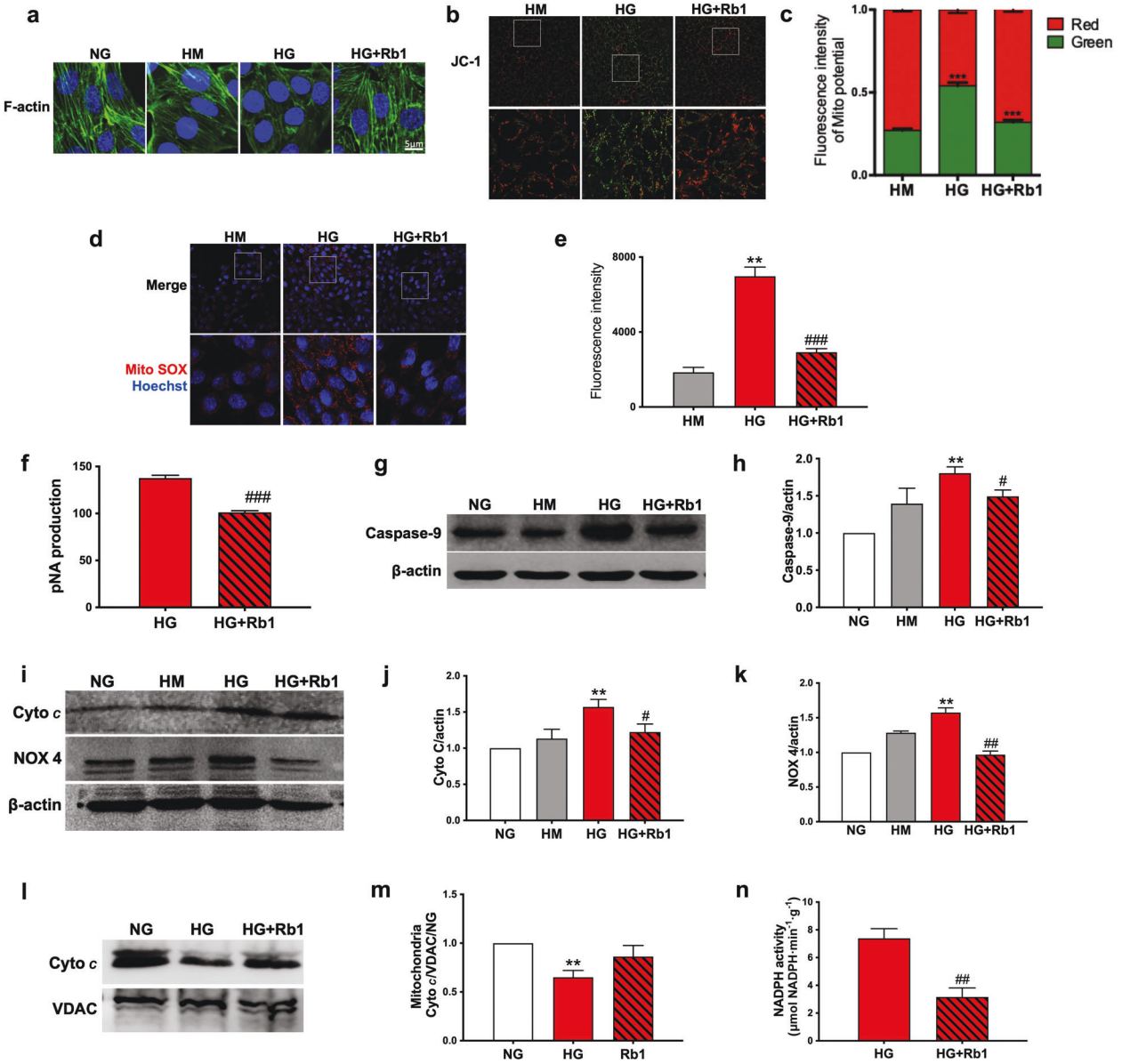

Fig. 2 Ginsenoside Rb1 improves mitochondrial damage and oxidative stress caused by high glucose. a Representative pictures of podocyte structure are shown. **b**, **c** Representative images of mitochondrial membrane potentials and their quantification are shown. **d**, **e** Representative images of ROS expression of podocytes and their quantification are shown. **f** The data represent the activity of Caspase-3 of each group. (**g**–**k**) We use Western blot to detect the expression level of (**g**, **h**) Caspase-9, (**i**, **j**) Cyto C and (**k**) NOX4. **l**, **m** The expression level of Cyto *c* in the mitochondria was detected by Western blotting, and VDAC served as a loading control. **n** The data indicate the activity of NADPH of each group. Data are shown as mean ± SEM. The differences among ≥3 groups were analyzed using ANOVA followed by the Bonferroni adjustment for multiple comparisons. *P* values between groups from unpaired *t* test of variance are as indicated. $^{**}P < 0.01$ versus NG/HM group. $^{\#}P < 0.05$, $^{\#\#}P < 0.01$, versus HG group.

Ginsenoside Rb1 combines with AR to protect mitochondria

Aldose reductase (AR) is an NADPH-dependent oxidoreductase and a key rate-limiting enzyme in the first step of the polyol pathway of glucose metabolism [24, 26–29]. The protein expression of AR in the HG group was significantly higher than that in the other groups, but ginsenoside Rb1 failed to reduce the expression of this protein (Fig. 3a, b). Therefore, we speculate that Rb1 might have changed the activity of AR and thereby induced a change in downstream NOX4.

The docking prediction results showed that the molecular docking score of human AR interacting with Rb1 was 5.9196, whereas that of mouse AR interacting with Rb1 was 5.3377. Moreover, the binding pattern diagram of the interaction between human and mouse-derived AR and Rb1 was obtained, and this analysis suggests that Rb1 binds to AR and exerts a certain inhibitory effect on AR activity (Fig. 3c, d).

To verify the above-described experimental results, AR activity was further detected and it was found that AR activity increased significantly under high-glucose conditions (Fig. 3e). Different doses of Rb1 (0.1, 1, 10 μM) were added after cell lysis to avoid the influence of factors such as intracellular metabolism. As a result, the activity of AR gradually decreased with increases in the dose of Rb1, which indicated that Rb1 can affect the activity of AR in a dose-dependent manner.

After that, in order to further explore the binding ability of Rg1 and R1 to AR, molecular docking was carried out, and the results showed that molecular docking scores of Rg1, R1 and mouse source AR interaction were 4.5210 and 4.3729, respectively

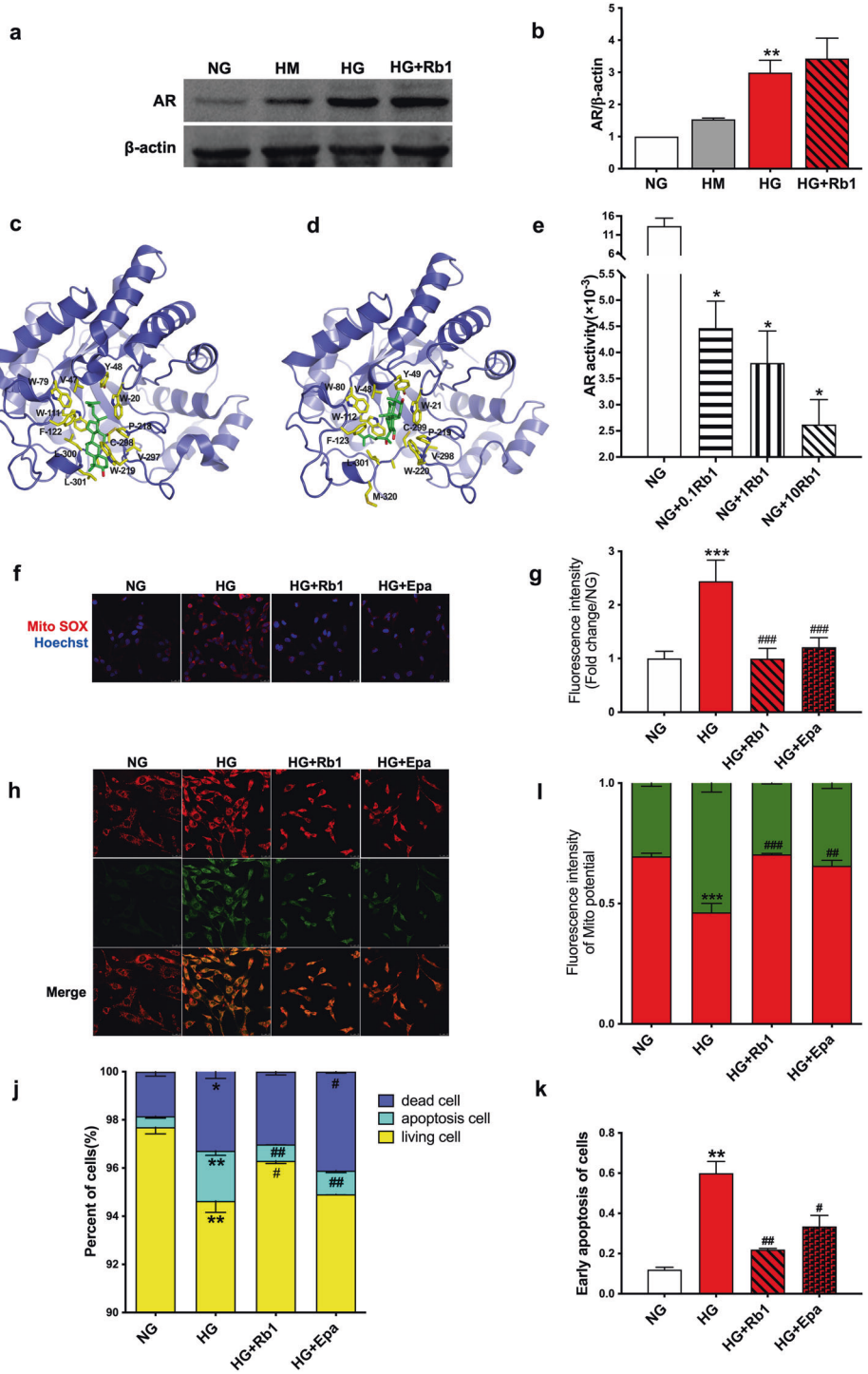

Fig. 3 Ginsenoside Rb1 combined with AR to protect mitochondrion. a, **b** Western blot was used to detect the expression of AR in cultured podocytes, and the representative pictures and their quantification are shown. **c** Pattern diagram of the interaction between human source AR and Rb1. **d** Pattern diagram of the interaction between mouse source AR and Rb1. **e** AR activity assay proved that ginsenoside Rb1 affects the activity of aldose reductase, the quantification is shown. **f**, **g** The mitochondrion-specific probe MitoSOX Red was used to detect changes in ROS levels, representative images and their quantification are shown. **h**, **i** Representative images of podocytes of mitochondrial membrane potentials and their quantification are shown. **j**, **k** Annexin V, FITC/PI was used to detect apoptosis, the quantifications are shown. Data are shown as mean ± SEM; The differences among ≥3 groups were analyzed using ANOVA followed by the Bonferroni adjustment for multiple comparisons. *P* values between groups from unpaired *t* test of variance are as indicated. $^{*}P < 0.05$, $^{**}P < 0.01$, $^{***}P < 0.001$, versus NG/HM group. $^{\#}P < 0.05$, $^{\#\#}P < 0.01$, $^{\#\#\#}P < 0.001$, versus HG group.

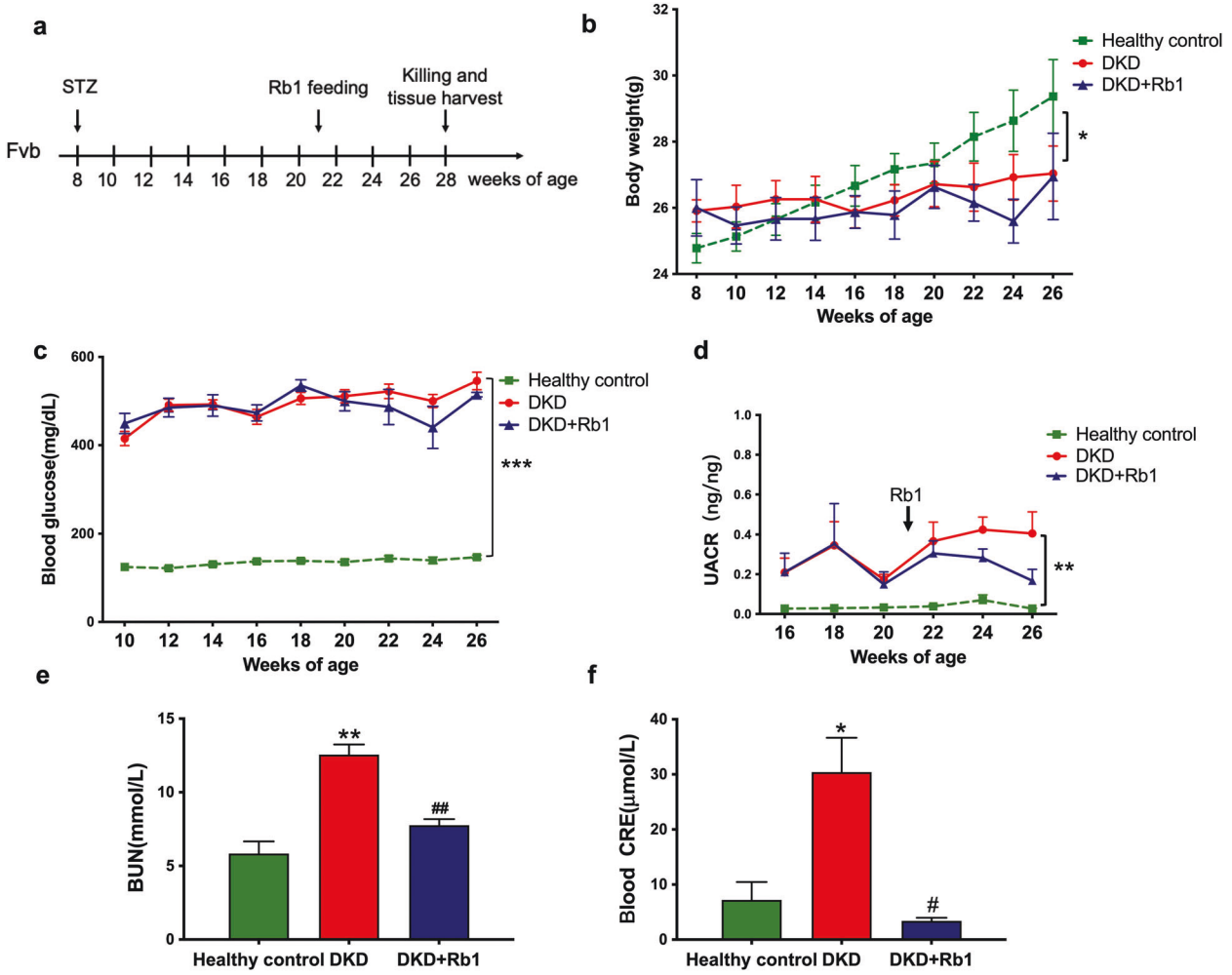

Fig. 4 Rb1 treatment attenuates UACR, blood BUN, and blood CRE in diabetic FVB mice. a Schema of study design. Healthy controls and diabetic FVB mice were monitored starting at 8 weeks of age. Vehicle or Rb1 (40 mg/kg) was administered each day starting at 21 weeks of age, and all mice were killed at 28 weeks of age. **b** Bodyweight of normal healthy controls (Health), vehicle-treated (DKD), and Rb1-treated diabetic FVB (DKD + Rb1) mice were monitored starting at 8 to 26 weeks of age. **c** Fasting blood glucose levels of mice were also monitored starting at 8 to 26 weeks of age. **d** Urinary albumin-to-creatinine ratio (UACR) of spot urine collected during the duration of the study is shown. (**e**) Blood BUN and (**f**) blood CRE were measured from the 24-h urine collected from mice at 28 weeks of age. *P* values between groups from unpaired *t* test of variance are as indicated. $^{*}P < 0.05$, $^{**}P < 0.01$, verHM grou/HM group. $^{\#}P < 0.05$, $^{\#\#}P < 0.01$, versus HG group.

(Supplementary Fig. S1). Therefore, compared with Rb1 (5.3377), the possibility of theoretical combination is relatively low, which further verifies the previous experimental results.

At the same time, Rb1 was compared with epalrestat, a currently recognized AR inhibitor [30–32]. The effects of epalrestat on oxidative stress and apoptosis were detected by MitoSOX fluorescence staining, JC-1 mitochondrial membrane potential assay, and Annexin V, FITC/PI kit (Fig. 3f–k). The results showed that epalrestat could effectively alleviate the mitochondrial membrane potential abnormalities and ROS overproduction induced by high glucose, but had a relatively weak effect on podocyte apoptosis compared to Rb1.

Ginsenoside Rb1 can mitigate diabetes-induced glomerular injury

To confirm whether ginsenoside Rb1 also plays a role in alleviating glomerular damage and improving renal function in model animals, FVB mice were used to establish a type 1 diabetes model. Eight-week-old FVB mice were intraperitoneally injected with STZ (50 mg/kg for 5 days) to induce type 1 diabetes, and starting 13 weeks later (i.e., 21-week-old mice), the mice received daily administrations of saline or ginsenoside Rb1 (40 mg/kg). The mice were sacrificed at 28 weeks of age, and blood, urine, and tissue samples were collected (Fig. 4a).

The results showed that Rb1 decreased the urine albumin creatine ratio (UACR), the blood levels of creatinine (CRE) and blood urea nitrogen (BUN) to a certain extent compared with the model group (Fig. 4b–g). Histological analysis showed that the diabetic mice exhibited significant glomerular hypertrophy and mesangial matrix expansion, and the mesangial volume fraction of the mice was significantly reduced after stimulation with ginsenoside Rb1 (Fig. 5a–c). Consistently, electron microscopic analysis of the model group showed obvious disappearance of the podocyte FPs and significant thickening of the GBM. However, ginsenoside Rb1 significantly alleviated these changes (Fig. 5d–f). Therefore, ginsenoside Rb1 alleviates diabetes-induced podocyte injury and effectively delays the progression of DKD in FVB mice.

Ginsenoside Rb1 inhibits the expression of multiple proteins in mice with DKD

In vivo experiments, the effect of Rb1 on apoptosis and ROS-related factors were verified again (Fig. 6). The combination of TUNEL staining (Fig. 6a), WT1 staining (Fig. 6b, c) and WB results

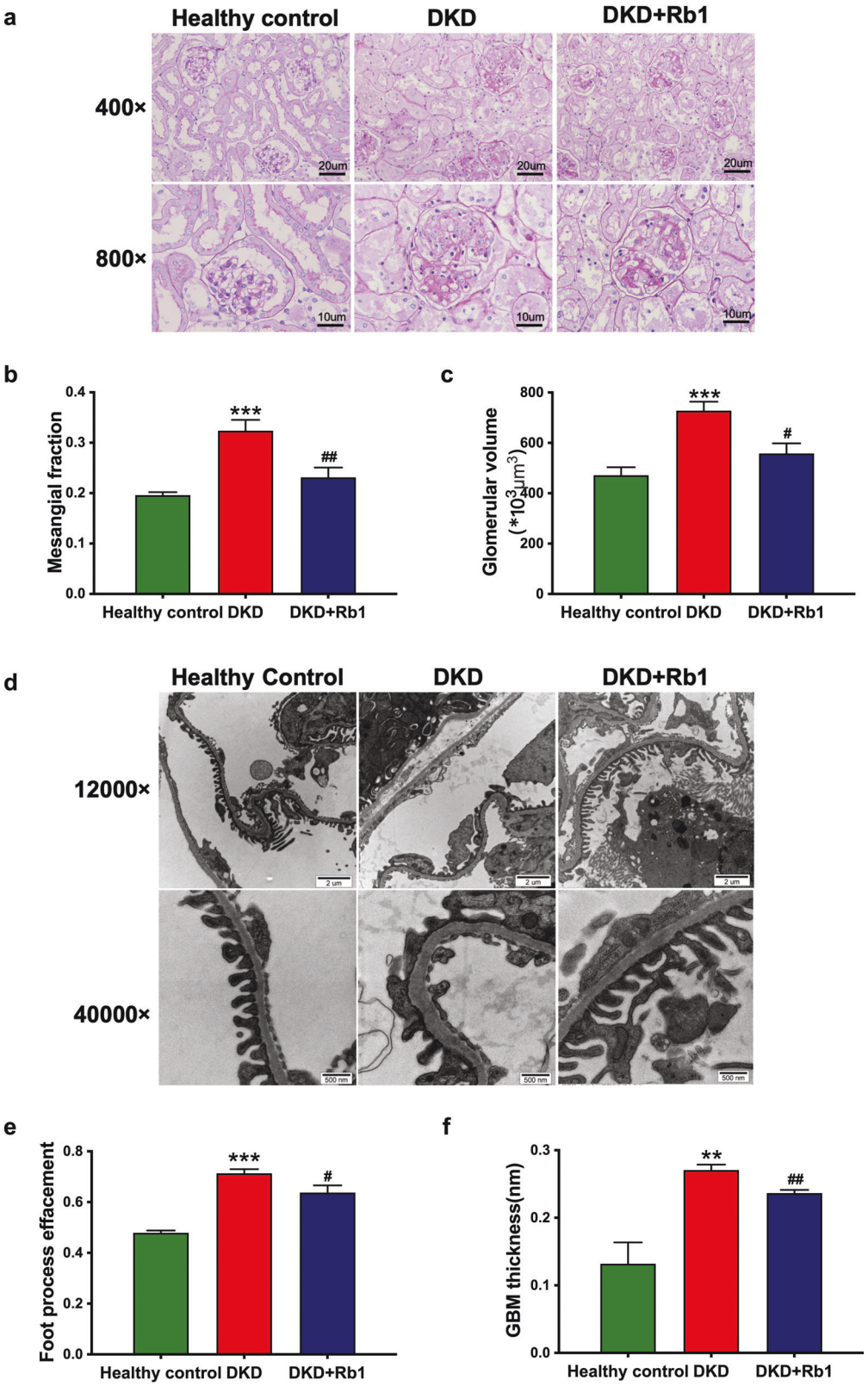

Fig. 5 Ginsenoside Rb1 can mitigate diabetes-induced glomerular injury. a Representative images of mouse kidneys stained with periodic acid–Schiff at 28 weeks of age are shown (top panels: original magnification ×400, bar = 20 μm; bottom panels: original magnification ×800, bar = 10 μm). Quantification of the fraction of mesangial area (**b**) and glomerular volume (**c**) are shown. **d** Electron microscopy was performed to assess ultrastructural changes in podocyte morphology (top panels: original magnification ×12,000; bottom panels: original magnification ×40,000). Representative images are shown. **e** Quantification of podocyte effacement. **f** Measurements of glomerular basement membrane (GBM) thickness. Data are shown as mean ± SEM; The differences among ≥3 groups were analyzed using ANOVA followed by the Bonferroni adjustment for multiple comparisons. *P* values between groups from unpaired *t* test of variance are as indicated. $^{**}P < 0.01$, $^{***}P < 0.001$, versus NG/HM group. $^{\#}P < 0.05$, $^{\#\#}P < 0.01$, versus HG group.

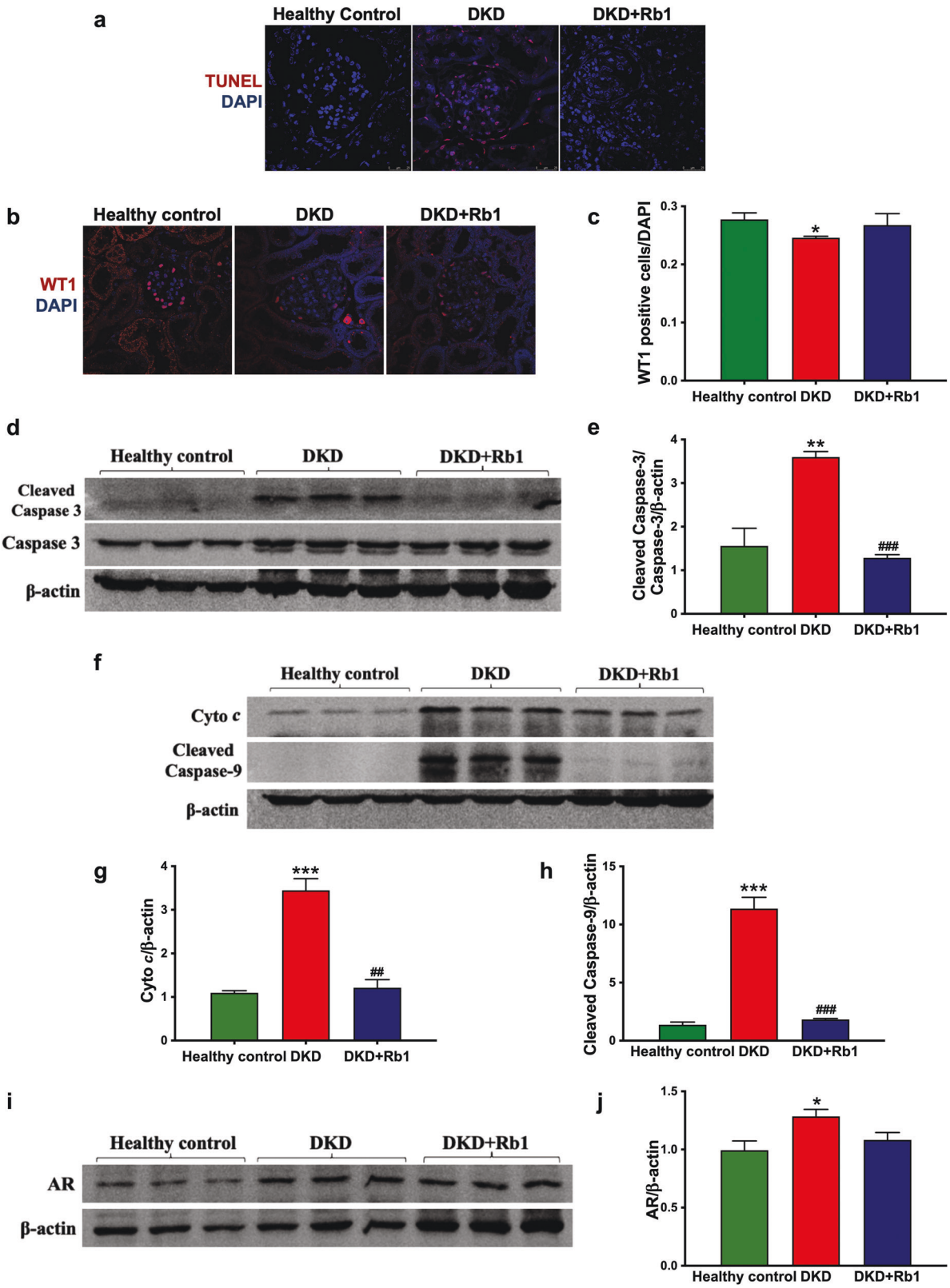

Fig. 6 Ginsenoside Rb1 inhibits the expression of multiple proteins in mice with diabetic kidney disease. a It shows a representative picture of the TUNEL staining results of each group, TUNEL-positive cells (red), DAPI (nuclear; blue). WT1 positive podocytes were counted (**c**) and representative pictures of TUNEL staining are shown (**b**), WT1-positive cells (red), DAPI (nuclear; blue). Western blot was used to detect the expression of (**d**, **e**) cleaved Caspase-3, (**f**–**h**) Cyto *c*, Caspase-9, and (**i**, **j**) AR in mice kidneys, and the representative pictures and their quantification are shown. Data are shown as mean ± SEM. The differences among ≥3 groups were analyzed using ANOVA followed by the Bonferroni adjustment for multiple comparisons. *P* values between groups from unpaired *t* test of variance are as indicated. $^{*}P < 0.05$, $^{**}P < 0.01$, $^{***}P < 0.001$, versus NG/HM group. $^{\#\#}P < 0.01$, $^{\#\#\#}P < 0.001$, versus HG group.

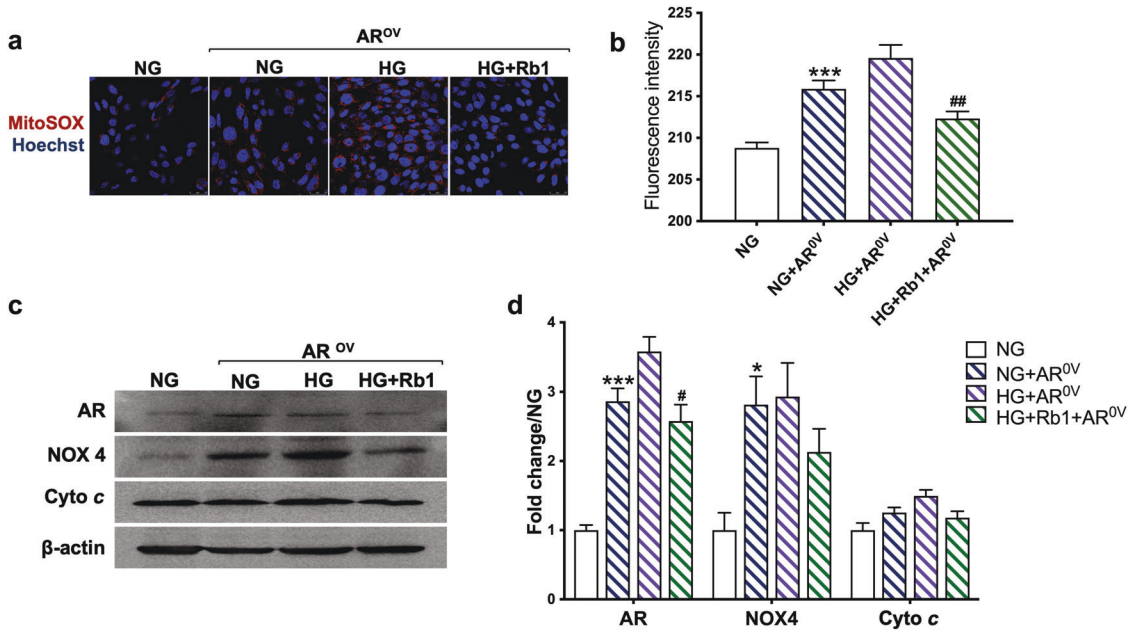

Fig. 7 Overexpression of AR alleviates oxidative stress. a, **b** MitoSOX Red was used to detect ROS production, representative images and their quantification are shown. **c**, **d** Western blot was used to detect the expression of AR, NOX4, and Cyto *c* in podocytes, and the representative pictures and their quantification are shown. Data are shown as mean ± SEM. *P* values between groups from unpaired *t* test of variance are as indicated. $^{*}P < 0.05$, $^{***}P < 0.001$, versus NG/HM group. $^{\#}P < 0.05$, $^{\#\#}P < 0.01$ versus HG group.

(Fig. 6d, e) confirmed that Rb1 can alleviate podocytes apoptosis in DKD, which was consistent with the previously mentioned in vitro protein results (Fig. 6f–j). These results indicated that Rb1 can inhibit the generation of ROS by binding to AR, alleviate the release of Cyto *c* in mitochondria induced by high glucose, prevent the activation of caspase 9, and the initiate the downstream caspase cascade, thereby achieving the effect of alleviating podocyte apoptosis.

Ginsenoside Rb1 alleviates oxidative stress in AR overexpression podocytes

In an attempt to further verify the relationship between AR and ginsenoside Rb1, podocytes were transfected with AR plasmid. The fluorescence staining results showed that AR overexpression significantly promoted the overproduction of ROS, and its effect was even more obvious than that of high glucose, and ginsenoside Rb1 can effectively inhibit it (Fig. 7a, b). Similarly, the expressions of AR and NOX4 proteins were consistent with the above results (Fig. 7c, d). However, after the over-expression of AR, there was no significant difference between the Cyto *c* in the NG group and the AR over-expression group, which might be related to the fact that Cyto *c* could be regulated by multiple factors, and a single factor could not have a huge impact on it.

DISCUSSION

Numerous evidences have confirmed the close relationship between hyperglycemia and kidney damage, but few effective drugs are currently available; thus, the identification of drugs that exert protective effects in the kidney is urgently needed. A lot of researches have indicated that Rb1 exerts a good relieving effect on myocardial diseases, retinopathy, and kidney damage caused by hyperglycemia, some studies have found that Rb1 may offer the most important medicinal contribution of the effective ingredients of *Panax notoginseng* [33–37]. Therefore, it can be speculated that Rb1 is a promising drug for diabetic nephropathy and related diseases, but its specific mechanism is unclear.

AR is an important enzyme that can convert glucose to sorbitol, particularly under hyperglycemic conditions [24, 26, 28, 31, 38]. In our study, we found that ginsenoside Rb1, an effective ingredient of *Panax notoginseng*, can combine with AR and inhibit its activity, and this inhibition can reduce the accumulation of sorbitol under high-glucose conditions and thus contribute to avoiding the subsequent occurrence of oxidative stress.

As a commonly used Chinese medicine, *Panax notoginseng* has been proven to alleviate diabetic nephropathy, but the specific mechanisms are unclear. The effects of *Panax notoginseng* preparation on patients with DKD have been evaluated by rigorous systematic reviews and meta-analyses of RCTS [39]. Compared with the conventional drug group, the conventional drug + *Panax notoginseng* preparation adjuvant therapy could reduce proteinuria and creatinine in DKD patients, but had no significant effect on the levels of fasting blood glucose and BUN. The results of proteinuria, serum creatinine level and blood glucose were basically consistent with the experimental results of this paper, while there were some differences in the BUN level. There are several possible reasons for the inconsistent results of blood urea nitrogen levels. The first reason is that the conventional drugs included in the analysis were different in each group, and the statistical results were heterogeneous. Secondly, the drugs used were not completely consistent. The drugs used in the RCT included in this meta-analysis were all preparation of *Panax notoginseng*, and there may be multiple active ingredients in the preparation, while the Rb1 was a monomer active ingredient with a relatively single effect. Finally, different degrees of disease, different subjects, different doses of drugs may all lead to the difference of the results.

The effect of a high glucose level on podocytes has been observed in a number of studies. In this study, we explored the effects of three main active ingredients of *Panax notoginseng*, namely, ginsenosides Rb1 and Rg1 and notoginsenoside R1 on apoptosis induced by high glucose through flow cytometry and WB, and found that Rb1 was the monomer with better effect. When Rb1 and AR were engaged in molecular docking, we also conducted docking with other two monomers, and the results showed that the molecular docking scores were all lower than Rb1. At present, we believe that the reason for this result is related to their different structures. Rb1 is 20(S)-protopanaxadiol, while

Rg1 and R1 are 20(S)-protopanaxatriol, which leads to the different pharmacological effects of the three.

Previous studies have noted that complex K containing ginsenoside Rb1 exerts an inhibitory effect on NOX4 expression [40], and we found that ginsenoside Rb1 also improves mitochondrial dysfunction by inhibiting the expression of NOX4. The detection of AR, which is the upstream regulatory factor of NOX4, revealed that ginsenoside Rb1 did not affect the expression of this protein and only affected its activity. Further studies on the binding sites between the two molecules revealed that ginsenoside Rb1 might bind to AR, which suggests that ginsenoside Rb1 might reduce AR activity by binding to AR and thereby alleviates the apoptosis of podocytes.

To verify whether ginsenoside Rb1 also plays a role in moderating glomerular damage and improving renal function in model animals, FVB mice were used for modeling type 1 diabetes. Compared with the DKD model group, the ginsenoside Rb1-treated group exhibited some improvements in mesangial matrix hyperplasia and FP fusion, which confirmed that ginsenoside Rb1 can alleviate glomerular injury in DKD. Moreover, the Western blot results showed that the expression of Caspase 3 and apoptosis-related protein Cyto *c* was also significantly decreased.

Shang et al reported that ginsenoside Rb1 induces the translocation and thus activation of GLUT1 and GLUT4 and affects glucose transport [17, 19]. However, the efficacy of its blood-glucose-lowering effect was not found in this study. This difference might be due to the shorter administration time, and the mice were modeled for a longer time and had a heavier weight.

This experiment also has some limitations. First of all, this article adopts daily intraperitoneal injection of STZ for 5 consecutive days to establish a type 1 diabetes model. Although this is the accepted method recommended by the AMDCC protocol, it still has certain defects. The non-specific toxicity of STZ may cause some damage to organs irrespectively of hyperglycemia, which may have some influence on the therapeutic effect of the drug. In addition, we mainly analyzed one active component of *Panax notoginseng* (ginsenoside Rb1), but the experimental results showed that although ginsenoside Rg1 and notoginseng R1 were less likely to bind with AR, they still had a certain alleviating effect on the renal injury induced by high glucose. However, the specific mechanism of action has not been further explored and studied in this study. And in the previous experiment, we chosed epalrestat, which is also an ARI, as a control group. Epalrestat is now mainly used for the treatment of diabetic peripheral neuropathy clinically, and the effects were most evident in subjects with better glycemic control and with no or mild microangiopathies [20]. In DKD, although several articles have mentioned that it could alleviate proteinuria in animal models and improve renal function, there is little support from relevant clinical literature [31, 32, 41, 42]. We speculate whether this difference may be related to the drug structure and metabolic pathway. In this article, we found that Rb1 can alleviate the damage of podocytes in DKD, and the effect is better than epalrestat. Since our experiments are currently limited to the animal level, there is no reliable clinical experimental data for reference.

In conclusion, Rb1 can bind to AR to inhibit its activity, as demonstrated with an AR activity detection kit and molecular docking tests, and can also reduce the expression of NOX4 to inhibit ROS generation, alleviate apoptosis, and ultimately relieve podocyte loss and apoptosis (Fig. 8). Further exploration of Rb1 and the interaction between Rb1 and AR might provide more therapeutic choices for DKD. At the same time, as an AR inhibitor, the role of Rb1 on other related complications of diabetes (such as diabetic peripheral neuropathy) is also worthy of more research and exploration.

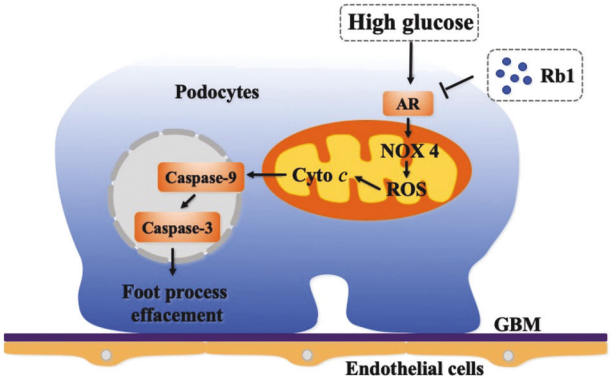

Fig. 8 Diagram of mechanism for Rb1 relieving hyperglycemia-induced glomerular podocyte injury. When podocytes were stimulated by high glucose, many organelles were damaged. The structure and function of mitochondria were abnormal and excessive ROS was produced, which eventually resulted in fusion and loss of foot processes. Rb1 can alleviate podocyte apoptosis by inhibiting the activity of AR, maintaining mitochondrial homeostasis and inhibiting the excessive production of ROS. Rb1, ginsenoside Rb1. GBM, glomerular basement membrane. ROS, Reactive Oxygen Species.

ACKNOWLEDGEMENTS

This work was supported by the National Key Research and Development Plan of China (2018YFC1704203), National Natural Science Foundation of China (81670671, 81870491, 82070741); Science & Technology Project of Beijing, China (D171100002817002); Fostering Fund of Chinese PLA General Hospital for National Distinguished Young Scholar Science Fund (2019-JQPY-002).

AUTHOR CONTRIBUTIONS

XMC, QH, and JYH designed research; JYH and BXC performed research; JYH wrote the paper; BXC, SYC, RL, and GYC participated in discussions and improvements related to the manuscript. JG and XMC directed the experiment.

ADDITIONAL INFORMATION

Supplementary information The online version contains supplementary material available at https://doi.org/10.1038/s41401-021-00788-0.

Competing interests: The authors declare no competing interests.

REFERENCES

1. Reidy K, Kang HM, Hostetter T, Susztak K. Molecular mechanisms of diabetic kidney disease. J Clin Invest. 2014;124:2333–40.
2. Association AD. Microvascular complications and foot care. Diabetes Care. 2018;41:S105–18.
3. Association AD. 10. Microvascular complications and foot care:standards of medical care in diabetes—2018. Diabetes Care. 2017;41:S105–18.
4. Torban E, Braun F, Wanner N, Takano T, Goodyer PR, Lennon R, et al. From podocyte biology to novel cures for glomerular disease. Kidney Int. 2019;96:850–61.
5. Weil EJ, Lemley KV, Mason CC, Yee B, Jones LI, Blouch K, et al. Podocyte detachment and reduced glomerular capillary endothelial fenestration promote kidney disease in type 2 diabetic nephropathy. Kidney Int. 2012;82:1010–7.
6. Ito Y, Hsu MF, Bettaieb A, Koike S, Mello A, Calvo-Rubio M, et al. Protein tyrosine phosphatase 1B deficiency in podocytes mitigates hyperglycemia-induced renal injury. Metabolism. 2017;76:56–69.
7. Wei X, Wei X, Lu Z, Li L, Hu Y, Sun F, et al. Activation of TRPV1 channel antagonizes diabetic nephropathy through inhibiting endoplasmic reticulum-mitochondria contact in podocytes. Metabolism. 2020;105:154182.
8. Pang HH, Li MY, Wang Y, Tang MK, Ma CH, Huang JM. Effect of compatible herbs on the pharmacokinetics of effective components of *Panax notoginseng* in Fufang Xueshuantong Capsule. J Zhejiang Univ-Science B. 2017;18:343–52.
9. Zhang Q, Xiao X, Li M, Li W, Yu M, Zhang H, et al. Attenuating effect of Fufang Xueshuantong Capsule on kidney function in diabetic nephropathy model. J Nat Med. 2012;67:86–97.
10. Yang CY, Wang J, Zhao Y, Shen L, Jiang X, Xie ZG, et al. Anti-diabetic effects of Panax notoginseng saponins and its major anti-hyperglycemic components. J Ethnopharmacol. 2010;130:231–6.
11. Tu QN, Dong H, Lu FE. Effects of panax notoginoside on the nephropathy in rats with type 1 diabetes mellitus. Chin J Integr Med. 2011;17:612–5.

12. Du YG, Wang LP, Qian JW, Zhang KN, Chai KF. *Panax notoginseng* saponins protect kidney from diabetes by up-regulating silent information regulator 1 and activating antioxidant proteins in rats. Chin J Integr Med. 2015;22:910–7.
13. Chen ZH, Li J, Liu J, Zhao Y, Zhang P, Zhang MX, et al. Saponins isolated from the root of panax notoginseng showed significant anti-diabetic effects in KK-Ay mice. Am J Chin Med 2008;36:939–51.
14. Sun W, Feng LY, Zhao ZJ, Liu TH, Yang MJ. Study on antioxidant effects and inhibition of podocyte apoptosis of PNS on DN rat (in Chinese). CJTCMP. 2011;26:1062–7.
15. Zhou JX, Ai ZM, Sun W, Wu LL, Qin LL, Li J, et al. Mechanism study of panax notoginseng saponins on protective effect for podocyte in diabetic nephropathy mice. China J Ttrad Chin Med Pharm. 2014;29:1316–21.
16. Shang W, Yang Y, Jiang B, Jin H, Zhou L, Liu S, et al. Ginsenoside Rb1 promotes adipogenesis in 3T3-L1 cells by enhancing PPARγ2 and C/EBPα gene expression. Life Sci. 2007;80:618–25.
17. Shang W, Yang Y, Zhou L, Jiang B, Jin H, Chen M. Ginsenoside Rb1 stimulates glucose uptake through insulin-like signaling pathway in 3T3-L1 adipocytes. J Endocrinol. 2008;198:561–9.
18. Ma X, Xie X, Zuo C, Fan J. Effects of ginsenoside Rg1 on streptozocin-induced diabetic nephropathy in rats (in Chinese). J Biomed Eng. 2010;27:342–7.
19. Shang W, Yang Y, Jiang B, Jin H, Zhou L, Liu S, et al. Ginsenoside Rb1 promotes adipogenesis in 3T3-L1 cells by enhancing PPARgamma2 and C/EBPalpha gene expression. Life Sci. 2007;80:618–25.
20. Hotta N, Akanuma Y, Kawamori R, Matsuoka K, Oka Y, Shichiri M, et al. Long-term clinical effects of epalrestat, an aldose reductase inhibitor, on diabetic peripheral neuropathy: the 3-year, multicenter, comparative aldose reductase inhibitor-diabetes complications trial. Diabetes Care. 2006;29:1538–44.
21. Crespo I, Giménez-Dejoz J, Porté S, Cousido-Siah A, Mitschler A, Podjarny A, et al. Design, synthesis, structure-activity relationships and X-ray structural studies of novel 1-oxopyrimido[4,5-c]quinoline-2-acetic acid derivatives as selective and potent inhibitors of human aldose reductase. Eur J Med Chem. 2018;152:160–74.
22. Jha JC, Banal C, Chow BSM, Cooper ME, Jandeleit-Dahm K. Diabetes and kidney disease: role of oxidative stress. Antioxid Redox Signal. 2016;25:657–84.
23. Toyoda M, Najafian B, Kim Y, Caramori ML, Mauer M. Podocyte detachment and reduced glomerular capillary endothelial fenestration in human type 1 diabetic nephropathy. Diabetes. 2007;56:2155–60.
24. Tang WH, Martin KA, Hwa J. Aldose reductase, oxidative stress, and diabetic mellitus. Front Pharmacol. 2012;3:87.
25. Paul M, Hemshekhar M, Kemparaju K, Girish KS. Berberine mitigates high glucose-potentiated platelet aggregation and apoptosis by modulating aldose reductase and NADPH oxidase activity. Free Radic Biol Med. 2019;130:196–205.
26. ElGamal H, Munusamy S. Aldose reductase as a drug target for treatment of diabetic nephropathy: promises and challenges. Protein Pept Lett. 2017;24:71–7.
27. Cohen MP. Aldose reductase, glomerular metabolism, and diabetic nephropathy. Metabolism. 1986;35:55–9.
28. Srivastava SK, Yadav UC, Reddy AB, Saxena A, Tammali R, Shoeb M, et al. Aldose reductase inhibition suppresses oxidative stress-induced inflammatory disorders. Chem-Biol Interact. 2011;191:330–8.
29. Santilli F, D'Ardes D, Davi G. Oxidative stress in chronic vascular disease: From prediction to prevention. Vascul Pharmacol. 2015;74:23–37.
30. Yama K, Sato K, Abe N, Murao Y, Tatsunami R, Tampo Y. Epalrestat increases glutathione, thioredoxin, and heme oxygenase-1 by stimulating Nrf2 pathway in endothelial cells. Redox Biol. 2015;4:87–96.
31. El Gamal H, Eid AH, Munusamy S. Renoprotective effects of aldose reductase inhibitor epalrestat against high glucose-induced cellular injury. BioMed Res Int. 2017;2017:1–11.
32. He J, Gao HX, Yang N, Zhu XD, Sun RB, Xie Y, et al. The aldose reductase inhibitor epalrestat exerts nephritic protection on diabetic nephropathy in *db/db* mice through metabolic modulation. Acta Pharmacol Sin. 2018;40:86–97.
33. Zhou P, Xie W, He S, Sun Y, Meng X, Sun G, et al. Ginsenoside Rb1 as an anti-diabetic agent and its underlying mechanism analysis. Cells. 2019;8:204.
34. Dong C, Liu P, Wang H, Dong M, Li G, Li Y. Ginsenoside Rb1 attenuates diabetic retinopathy in streptozotocin-induced diabetic rats. Acta Cir Bras. 2019;34: e201900201.
35. Qin L, Wang J, Zhao R, Zhang X, Mei Y. Ginsenoside-Rb1 improved diabetic cardiomyopathy through regulating calcium signaling by alleviating protein O-GlcNAcylation. J Agric Food Chem. 2019;67:14074–85.
36. Nan F, Sun G, Xie W, Ye T, Sun X, Zhou P, et al. Ginsenoside Rb1 mitigates oxidative stress and apoptosis induced by methylglyoxal in SH-SY5Y cells via the PI3K/Akt pathway. Mol Cellular Probes. 2019;48:101469.
37. Pintusophon S, Niu W, Duan XN, Olaleye OE, Huang YH, Wang FQ, et al. Intravenous formulation of Panax notoginseng root extract: human pharmacokinetics of ginsenosides and potential for perpetrating drug interactions. Acta Pharmacol Sin. 2019;40:1351–63.
38. So WY, Wang Y, Ng MC, Yang X, Ma RC, Lam V, et al. Aldose reductase genotypes and cardiorenal complications: an 8-year prospective analysis of 1,074 type 2 diabetic patients. Diabetes Care. 2008;31:2148–53.
39. Tang X, Huang M, Jiang J, Liang X, Li X, Meng R, et al. Panax notoginseng preparations as adjuvant therapy for diabetic kidney disease: a systematic review and meta-analysis. Pharm Biol. 2020;58:138–45.
40. Song W, Wei L, Du Y, Wang Y, Jiang S. Protective effect of ginsenoside metabolite compound K against diabetic nephropathy by inhibiting NLRP3 inflammasome activation and NF-kappaB/p38 signaling pathway in high-fat diet/streptozotocin-induced diabetic mice. Int Immunopharmacol. 2018;63:227–38.
41. Iso K, Tada H, Kuboki K, Inokuchi T. Long-term effect of epalrestat, an aldose reductase inhibitor, on the development of incipient diabetic nephropathy in Type 2 diabetic patients. J Diabetes Complications. 2001;15:241–4.
42. Hotta N, Kawamori R, Fukuda M, Shigeta Y. Aldose Reductase Inhibitor-Diabetes Complications Trial Study G. Long-term clinical effects of epalrestat, an aldose reductase inhibitor, on progression of diabetic neuropathy and other microvascular complications: multivariate epidemiological analysis based on patient background factors and severity of diabetic neuropathy. Diabet Med. 2012;29:1529–33.